Increased Substrate Stiffness Elicits a Myofibroblastic Phenotype in Human Lamina Cribrosa Cells

Response of Lamina Cribrosa Cells to Environmental Mechanical Cues

Baiyun Liu[1,2], Jason I. Kilpatrick[2], Bartlomiej Lukasz[2], Suzanne P. Jarvis[1,2], Fiona McDonnell[3], Deborah M. Wallace[3], Abbot F. Clark[5] and Colm J. O'Brien[3,4]

[1]School of Physics, Conway Institute, University College Dublin, Belfield, Dublin 4, Ireland

[2]Conway Institute of Biomolecular and Biomedical Science, University College Dublin, Belfield, Dublin 4, Ireland

[3]School of Medicine, University College Dublin, Belfield, Dublin 4, Ireland

[4]Department of Ophthalmology, Mater Misericordiae University Hospital, Dublin 7, Ireland

[5]North Texas Health Science Center, Ft. Worth, Texas, United States of America

Keywords: Substrate stiffness; Myofibroblast transformation; Lamina cribrosa cells; Biophysical cues; Glaucoma

- Supporting Material –

Corresponding Author: Prof. Colm J. O'Brien, FRCS, MD, Department of Ophthalmology, Mater Misericordiae University Hospital, 60 Eccles Street, Dublin 7, Ireland.; cobrien@mater.ie

SI TEXT

AFM characterization of silicone elastomer substrates. Force spectroscopy measurements were performed on substrates before fibronectin coating based on the values provided from the manufacturer. Thick homogeneous gels around 90 μm in thickness were tested with sphere-tipped cantilevers. A spherical colloidal tip was prepared by manually gluing a glass bead (≈ 9 μm in diameter, Whitehouse Scientific Ltd) to the end of CSC38-Tipless ($k \approx 0.06$ N m^{-1}) for soft substrates and NSC12-Tipless ($k \approx 0.35$ N m^{-1}) for stiff substrates using two-part epoxy (EPO-TEK 353ND, Epoxy Technology Inc.). The force *vs.* indentation data were performed over a peak force range of 4 nN to 20 nN at a probe displacement rate of 0.6 μm s^{-1}. Before each experimental measurement, the exact spring constant was determined for each lever using the Sader method[1] in air. Inverse Optical Lever Sensitivity (InvOLS) was subsequently measured in PBS using a rigid glass substrate as a reference. Due to the large adhesion force between the tip and soft sample, the elastic modulus of the substrates was determined based on a model including the adhesive interactions between the AFM tip and sample surfaces (Johnson-Kendall-Roberts (JKR) model).[2] Elastic modulus data are reported as mean ± standard deviation (n_{curves} = 50/sample) (Figure S1).

Determining Cells' Young's Modulus with AFM

For live cell measurements, cells are first localized using an optical system, a cone shaped probing cantilever ($k \approx 0.03$ N m^{-1}) is then brought in close proximity with a studied cell over the cell body (avoiding the nucleus and the cell edge) (Figure S3A). Force map array (12 × 12) were collected which contains individual force displacement curves distributed equally over the selected region. The use of cone-shape tip has the extraordinary ability of mapping local elastic properties over the entire cell surface, instead of obtaining an average elastic cell response as is the case when using spherical bead. Care is taken to make sure that the indentation force does not rupture the cell membrane and lead to cell death. These force curves are subsequently converted into force-versus-indentation curves, which describe the depth dependent mechanical response to the applied load. The Young's modulus value, characterizing the cell stiffness was then evaluated within the Hertzian contact mechanics, taking into account an infinitely stiff indenter with a selected geometry of the AFM tip.

For a conical indenter:

$$F_{cone} = \frac{2}{\pi}\frac{E}{(1-\nu^2)}\tan\alpha\,\delta^2 \qquad (1)$$

This expression is a particular case of the generalized Hertzian contact theory[3] developed by Sneddon,[4] where E and v are the local Young's modulus and Poisson's ratio, respectively, and α is the opening angle of the probing tip. An empirical algorithm was developed to facilitate a robust automated determination of the point of contact as this has been shown a critical parameter in determining the *E* value. Following each fit, all force curves thus generate an elasticity map representing the variation of local cell stiffness within the measured region (Figure S3B). Due to the spread morphology of cells on the substrate, representative cell stiffness points were selected to demonstrate the apparent difference in *E*: point (a) locates near the soft cell nucleus region, point (b) represents intermediate cytoplasma region and point (c) shows peripheral cell region maybe composed of actin structure that has is 25 and 9 times stiffer in comparison with point (a), (b), respectively (Figure S3C). Since the Young's modulus values were not normally distributed according to the Shapiro-Wilks test ($p < 0.05$), and were therefore log-transformed to better illustrate stiffness distribution for a cell (Figure S3D).

Integrating Confocal Microscopy with AFM imaging

Combining AFM with other optical techniques allows for a more comprehensive study of biological systems. In this study, a combined phase contrast image (Figure S4A) and FITC image taken of AFM cantilever and α-SMA labelled (green) glaucoma LC cells on the soft substrate. Cells were fixed using 4% paraformaldehyde and imaged in PBS. The AFM cantilever (DNP-10 tip C, $k \approx 0.32$ N m^{-1}) is positioned above cell membrane of selected area. The confocal image is imported into the Igor pro software (WaveMetrics, USA) and AFM fields of view are selected on the fluorescent image. Features which appear in both imaging modalities (e.g., cell borders) are used as fiduciary markers such that both images are overlaid. During imaging the AFM tip indents the cell membrane, producing deflection images in which the stiffer sub-membrane structures appear elevated, and in this way, facilitate the acquisition of high-resolution images, providing structural resolution on the nanoscale. Figure S4C (height images) and Figure S4D (amplitude images) were recorded using AFM in tapping mode. Amplitude images can be correlated with confocal images of the α-SMA for an 60 × 60μm field of view. This allows a direct correlation of stress fibre structure with nano-scale topographic features for LC cells.

Data Analysis

A Multifactor between-subjects ANOVA was applied to test the main and interaction effects of all three independent variables[5] in RStudio (Version 1.1.383). The study was conducted using a 2 (normal or glaucoma) x 2 (soft or stiff) x 3 (donor number) between-subjects factorial design). The dependent variable was cell circularity. A *p* value of less than 0.05 was considered significant.

SUPPORTING FIGURES

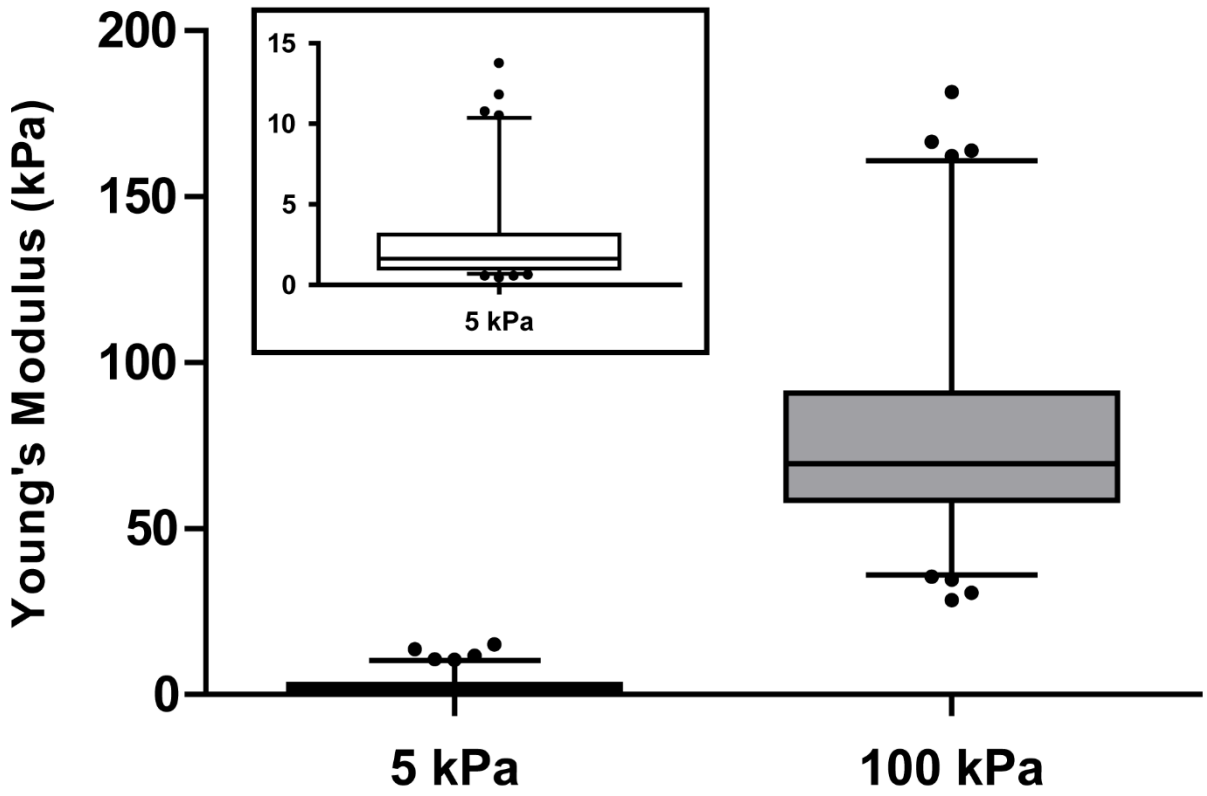

Figure S1. Substrate characterization using AFM. The measured elastic (Young's) modulus (E) values for the commercial soft (5 kPa) and stiff (100 kPa) substrates were 3.13 ± 3.80 kPa and 78.84 ± 35.51 kPa, respectively.

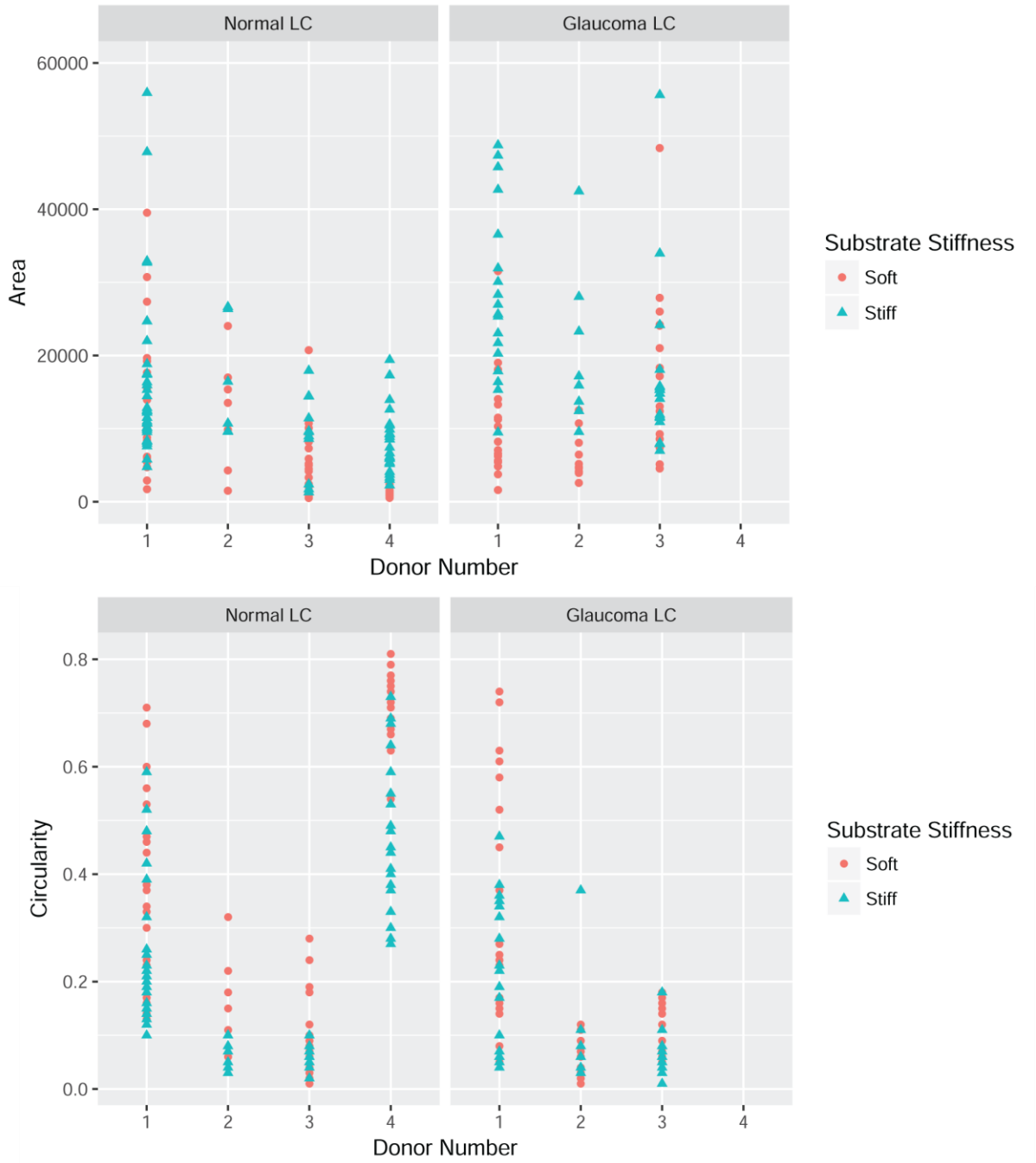

Figure S2. Comparison of cell area and circularity among different donors. Overall, 4 normal donors and 3 glaucoma donors were investigated in this study. Scatter plots show the distribution of parameters for individual donor numbers. Briefly, stiffness substrates induced a greater cell area (upper part of the scatter plot) and a smaller circularity (bottom part of the scatter plot). By applying the multifactor between-subject ANOVA, the design of the model includes the main effect of donor number, diagnosis, substrate stiffness and the interaction effect of donor * diagnosis, donor * stiffness, and diagnosis * stiffness. The AVOVA result demonstrated the significant effect of substrate stiffness in cell circularity but not the diagnosis. This is due to the high correlation of diagnosis and donor number. A larger sample size would be required to reveal any statistically significant effect of diagnosis. The statistic output from RStudio (Version 1.1.383) is attached as Table S1.

Table S1 Statistic output of circularity data from RStudio (Version 1.1.383)

	Df	Sum of Squares	Mean Square	F	*P* value
Donor Number	5	6.641	0.3084	86.751	< 0.001
Diagnosis					
Substrate stiffness	1	0.375	0.375	24.512	< 0.001
Donor * Substrate stiffness	1	0.3736		4.0664	< 0.001
Residuals	224	3.4297			

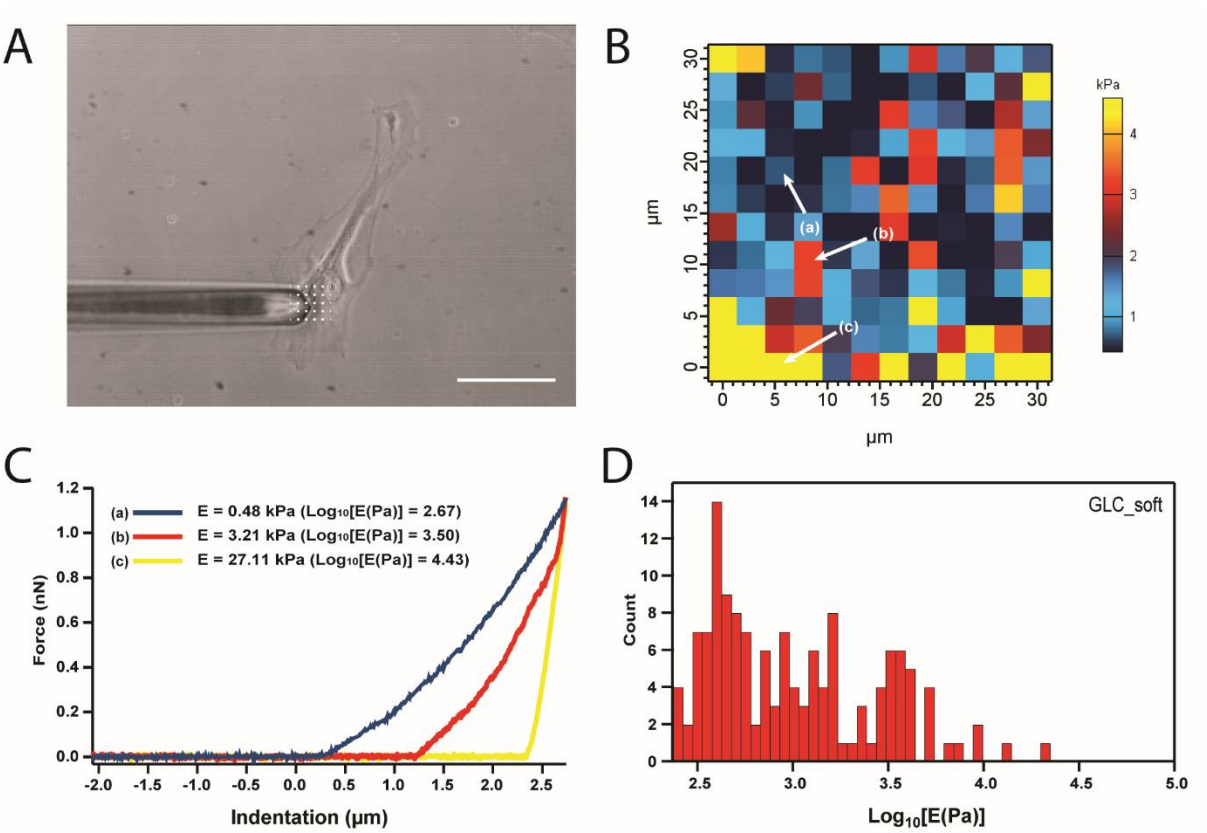

.

Figure S3. AFM indentation set up for live primary human glaucoma LC cells cultured on a soft substrate. A: phase-contrast image shows the rectangular AFM cantilever with cone-shape tip was navigated over a defined region near nucleus using light microscopy. For every specimen, 12 x 12 points were probed in a 30 x 30 µm region. Scale bar: 80 µm. B: Color-coded elasticity map extracted from fitting each approach curves into the Sneddon model. Points (a)-(c) represent cell body, intermediate region and peripheral region, respectively. C: Force-indentation curves and their respective E and Log (E) measured in the marked point for this specimen. D: Log(E) histogram exhibiting a non-normal distribution (p<0.001, Shapiro-Wilks test) with multiple peaks.

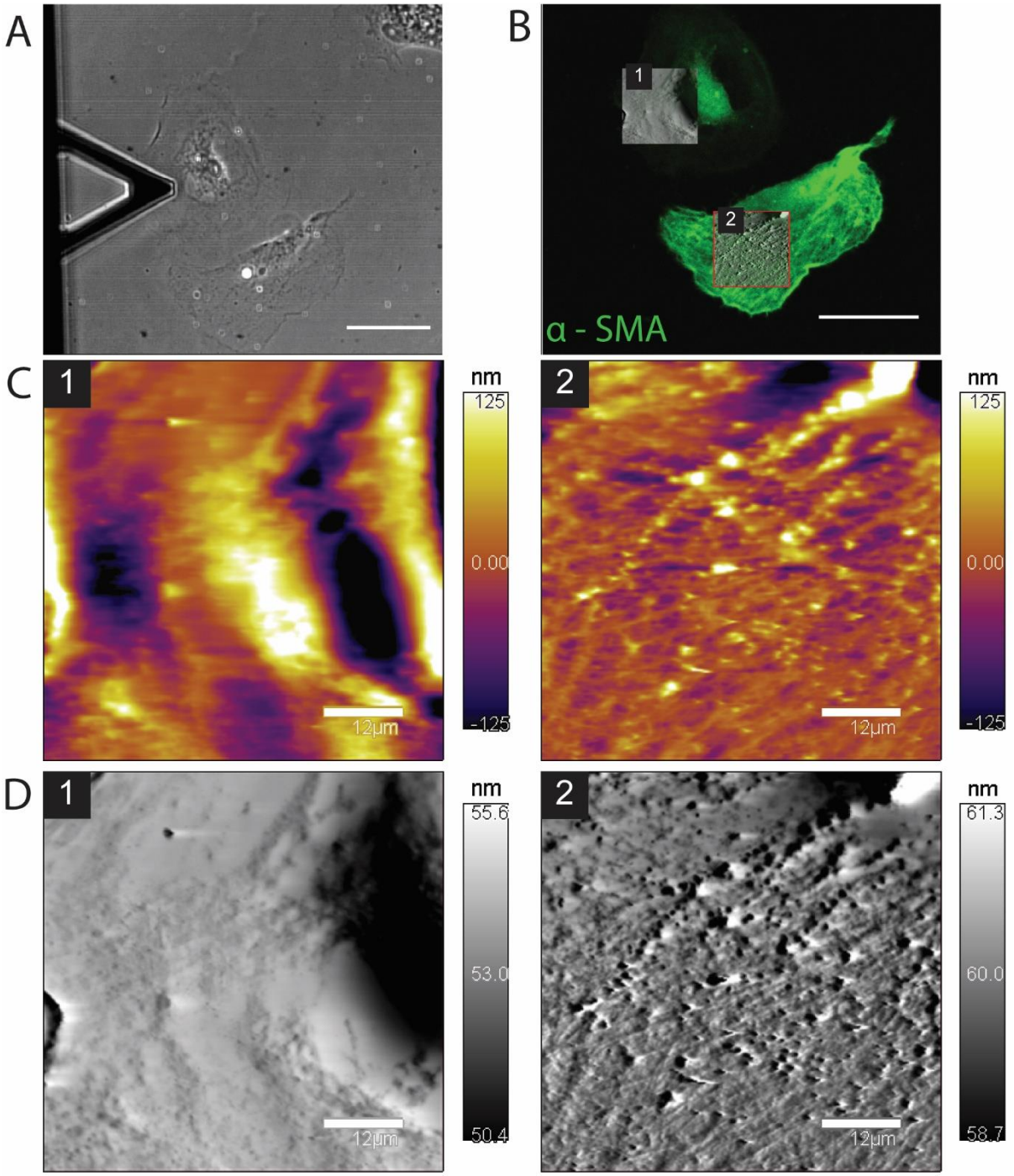

Figure S4. Integrated AFM and Confocal microscopy assessment of the glaucoma LC cell morphological features on soft substrates. A: The phase-contrast image from top view camera used to position the AFM triangular cantilever with sharp tip over the stained cells. B: Fluorescent image of studied cells stained with myofibroblast marker α-SMA (green) overlaid with AFM images. Scale bar: 80 µm. AFM height (C) and amplitude (D) images were taken in regions 1 and 2. Scale bar: 12 µm. α-SMA-negative cell (1) exhibited relatively smooth curved surfaces, in contrast, α-SMA-positive cell (2) showed a remarkably rougher surface, indicative of actin stress fibers. All images were processed using a third-order plane-fit function.

References

1. Sader JE, Chon JW, Mulvaney P. Calibration of rectangular atomic force microscope cantilevers. Rev Sci Instrum 1999;70:3967-3969.
2. Johnson K, Kendall K, Roberts A. Surface energy and the contact of elastic solids. *Proc R Soc Lond A Math Phy Eng Sci*: The Royal Society; 1971:301-313.
3. Hertz H. Uber den kontakt elastischer korper. J Reine Angew Mathematik 1881;92:245-260.
4. Sneddon IN. The relation between load and penetration in the axisymmetric Boussinesq problem for a punch of arbitrary profile. Int J Eng Sci 1965;3:47-57.
5. DeCoster, Jamie. "Testing group differences using t-tests, ANOVA, and nonparametric measures." Accessed November; 2006;30: 202006-0.